

## RESEARCH ARTICLE

10.1002/2016PA003048

## Key Points:

- The global seawater Mo-isotope composition during the early stages of the T-OAE was constant
- Sedimentary Mo-isotope fluctuations in Yorkshire during the early stages of the T-OAE record local hydrographic phenomena
- Stratigraphic changes in Mo-isotope compositions suggest a secular decline in global anoxia following the T-OAE

## Correspondence to:

A. J. Dickson,  
alex.dickson@earth.ox.ac.uk

## Citation:

Dickson, A. J., B. C. Gill, M. Ruhl, H. C. Jenkyns, D. Porcelli, E. Idiz, T. W. Lyons, and S. H. J. M. van den Boorn (2017), Molybdenum-isotope chemostratigraphy and paleoceanography of the Toarcian Oceanic Anoxic Event (Early Jurassic), *Paleoceanography*, 32, 813–829, doi:10.1002/2016PA003048.

Received 18 OCT 2016

Accepted 22 JUN 2017

Accepted article online 27 JUN 2017

Published online 10 AUG 2017

## Molybdenum-isotope chemostratigraphy and paleoceanography of the Toarcian Oceanic Anoxic Event (Early Jurassic)

Alexander J. Dickson<sup>1</sup> , Benjamin C. Gill<sup>2</sup> , Micha Ruhl<sup>1</sup> , Hugh C. Jenkyns<sup>1</sup> , Donald Porcelli<sup>1</sup> , Erdem Idiz<sup>1</sup>, Timothy W. Lyons<sup>3</sup> , and Sander H. J. M. van den Boorn<sup>4</sup>
<sup>1</sup>Department of Earth Sciences, University of Oxford, Oxford, U.K., <sup>2</sup>Department of Geosciences, Virginia Polytechnic Institute and State University, Blacksburg, Virginia, USA, <sup>3</sup>Department of Earth Sciences, University of California, Riverside, California, USA, <sup>4</sup>Shell Global Solutions International, Rijswijk, Netherlands

**Abstract** Molybdenum (Mo)-isotope chemostratigraphy of organic-rich mudrocks has been a valuable tool for testing the hypothesis that the Toarcian Oceanic Anoxic Event (T-OAE, Early Jurassic, ~183 Ma) was characterized by the spread of marine euxinia (and organic matter burial) at a global scale. However, the interpretation of existing Mo-isotope data for the T-OAE (from Yorkshire, Cleveland Basin, U.K.) is equivocal. In this study, three new Mo-isotope profiles are presented: from Dotternhausen Quarry (South German Basin, Germany), the Rijswijk core (West Netherlands Basin, Netherlands), and the Dogna core (Belluno Basin, northern Italy). Precise biostratigraphic and chemostratigraphic correlation between the three sites allows a direct comparison of the data, enabling some key conclusions to be reached: (i) The Mo-isotope composition of seawater during the peak of the T-OAE was probably close to ~1.45‰, implicating a greater removal flux of sulphides from seawater, and a larger extent of global seafloor euxinia compared to the present day; (ii) Mo-isotope cycles previously identified in the Yorkshire sedimentary succession are attributed to changes in the degree of local Mo drawdown from overlying Cleveland Basin seawater; (iii) The consistency of the new multisite Mo-isotope data set indicates a secular reduction in the burial of Mo globally in the late stages of the T-OAE, implying a contraction in the extent of global marine euxinia; (iv) Subtle differences in the Mo-isotope composition of deposits formed in different euxinic subbasins of the European epicontinental shelf were probably governed by local variations in basin hydrography and rates of water renewal.

## 1. Introduction

The Early Jurassic Toarcian stage was characterized by the deposition of mudrocks enriched in organic matter in many marine sedimentary successions worldwide. The wide distribution of age-equivalent lower Toarcian black shales from northern and southern Europe [Jenkyns, 1988; Jenkyns *et al.*, 2002], South America [Al-Suwaidi *et al.*, 2010, 2016], Japan [Gröcke *et al.*, 2011; Kemp and Izumi, 2014], western Canada and Siberia [Caruthers *et al.*, 2011; Suan *et al.*, 2011], Tibet [Fu *et al.*, 2016], and elsewhere suggests that enhanced organic matter burial was principally controlled by a global set of environmental drivers and therefore constitutes a global Oceanic Anoxic Event (commonly termed the “T-OAE” [Jenkyns, 1988; van der Schootbrugge *et al.*, 2005]). The T-OAE can be chemostratigraphically defined not only by the stratigraphic extent of organic-rich sediments but also by a broad positive carbon-isotope excursion that was primarily caused by enhanced global deposition of organic matter. This positive excursion was punctuated by an abrupt negative carbon-isotope excursion in marine and terrestrial organic matter [Hesselbo *et al.*, 2000, 2007]. This negative carbon-isotope excursion likely records the injection of isotopically light carbon into the oceans and atmosphere, either from the dissociation of methane hydrates [e.g., Hesselbo *et al.*, 2000], magmatic intrusions into organic-rich sediments [McElwain *et al.*, 2005], and/or volcanic activity associated with the Karoo-Ferrar large igneous province [Pálfi and Smith, 2000; Svensen *et al.*, 2007; Percival *et al.*, 2015]. Overall, the significance of the T-OAE is manifested in a carbon-cycle perturbation that reflects changes in climate and biogeochemical cycling at a global scale [Jenkyns, 2010]. In terms of north European ammonite stratigraphy, the negative carbon-isotope event can be considered to have lasted from the late *tenuicostatum* Zone to the mid-*falciferum* (or *serpentinum*) Zone.

The isotopic composition of the trace metal molybdenum (Mo), which was previously measured in mudrock samples from the Jet Rock in Yorkshire, England (Cleveland Basin [Pearce *et al.*, 2008]) has been used to

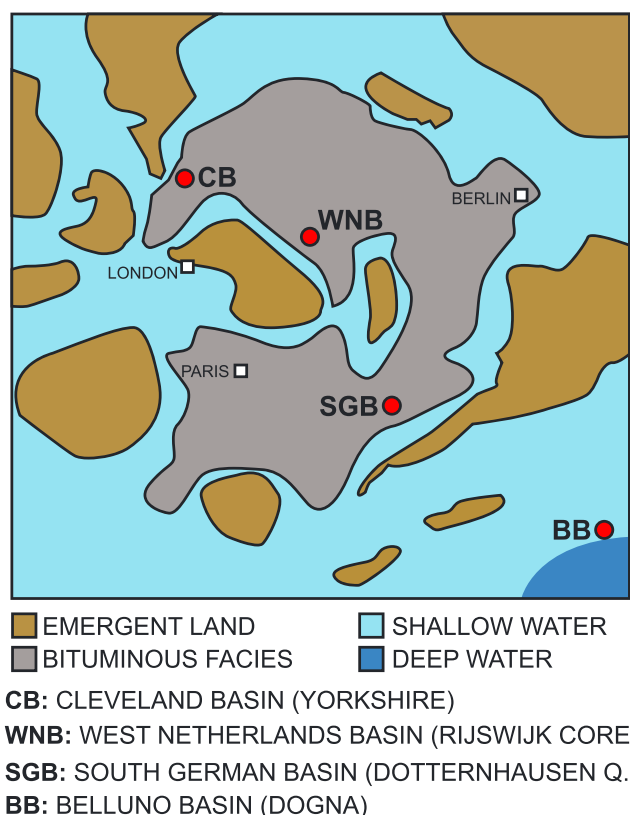


**Figure 1.** Paleogeographic map of the European continental shelf and Tethyan continental margin, modified from Ziegler [1982]. Study locations are marked in red.

support the argument of a greater extent of marine euxinia during the T-OAE compared to the present day. Mo is conservative in seawater today [Nakagawa *et al.*, 2012] and has a relatively long residence time of ~440 kyr [Miller *et al.*, 2011]. The isotopic composition of Mo is reported as parts per thousand deviations from the NIST 3134 international standard, plus 0.25‰:

$$\delta^{98/95}\text{Mo} = \left( \left( \frac{{}^{98}\text{Mo}}{{}^{95}\text{Mo}}_{\text{sample}} - \frac{{}^{98}\text{Mo}}{{}^{95}\text{Mo}}_{\text{NIST 3134}} \right) / \frac{{}^{98}\text{Mo}}{{}^{95}\text{Mo}}_{\text{NIST 3134}} \right) \times 1000 + 0.25 \quad (1)$$

$\delta^{98/95}\text{Mo}$  in modern seawater is homogenous with a value of 2.34‰ [Nakagawa *et al.*, 2012] and is controlled by the balance between the amount and isotopic composition of Mo entering the world oceans, mainly via rivers, and the mass and composition of Mo being removed from the world ocean by incorporation into sediments. Variations in the seawater Mo-isotope composition in the past have occurred because the redox-dependent removal fluxes into marine sediments were altered. In oxic and suboxic environments, the lighter Mo isotopes are mainly removed by adsorption to Mn-oxyhydroxide minerals, with compositions that are typically 3‰ lighter than seawater [Siebert *et al.*, 2003; Barling and Anbar, 2004; Goldberg *et al.*, 2009; Wasylenki *et al.*, 2011]. Conversely, in environments characterized by the presence of reduced sulphur ( $\text{H}_2\text{S}$ ) in seawater and sediment pore waters, Mo is removed from solution by the formation of Mo sulphides (thiomolybdates) [Eriksson and Helz, 2000], with an isotopic composition ~0.90 to 0.50‰ less than local seawater (as observed in modern marine sediments [Poulson *et al.*, 2006; Poulson-Brucker *et al.*, 2009, 2012; Nägler *et al.*, 2011]). Any change in the balance of Mo removal fluxes between oxic and/or sulphidic sediments has a direct impact on the globally homogenous seawater isotopic composition, with a greater proportion of Mo removed into sulphidic sediments resulting in a lighter seawater Mo-isotope composition. Tracing the Mo-isotope composition of global seawater can thus be used to monitor global changes in the balance of oxic versus sulphidic sedimentation.

The Mo-isotope composition of open ocean or global seawater can be recorded by sediments deposited in highly restricted sulphidic environments with dissolved aqueous  $\text{H}_2\text{S}$  concentrations  $> \sim 11 \mu\text{mol/l}$  [Helz

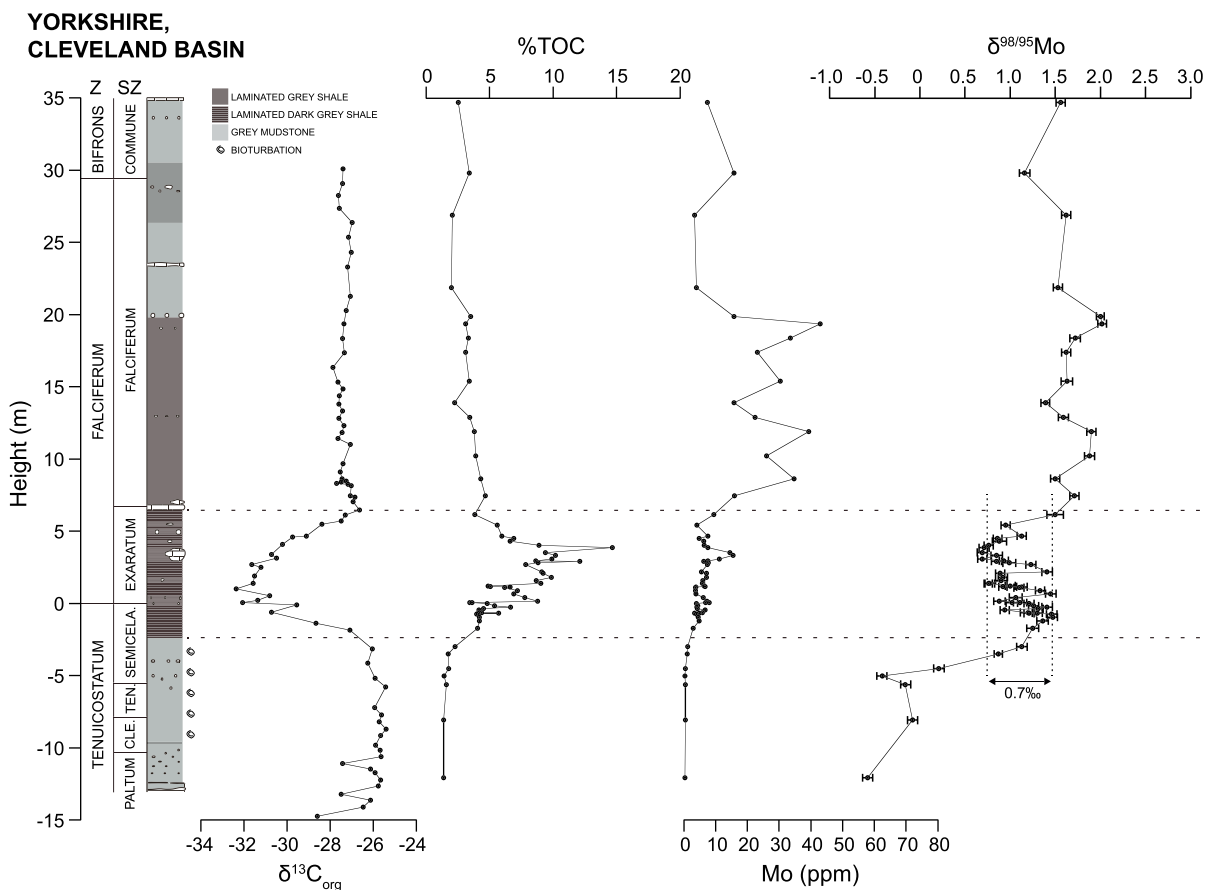


**Figure 2.** Geochemical data from Yorkshire, UK (Port Mulgrave, Saltwick Bay, and Hawsker Bottoms). Ammonite stratigraphy is from *Howarth* [1973, 1992], carbon isotopes and TOC are from *Cohen et al.* [2004] and *Kemp et al.* [2005], and Mo isotopes and concentrations are from *Pearce et al.* [2008]. Vertical dashed lines highlight the range of the Mo-isotope fluctuations observed by *Pearce et al.* [2008] in the lower *falciferum* ammonite Zone. Z: Ammonite zones. SZ: Ammonite subzones. Cle.: Clevelandicum Subzone. Ten.: *tenuicostatum* Subzone. Semicela.: *semicelatum* Subzone. Zone abbreviations are the same in Figures 3–7. Lithologic log adapted from *Pearce et al.* [2008].

*et al.*, 1996; *Eriksson and Helz*, 2000; *Neubert et al.*, 2008], where more than 90% of the dissolved Mo inventory has been removed into the accumulating sediments (termed “quantitative drawdown”). This behavior allows the sedimentary isotopic composition to approach that of the initial open ocean seawater composition (i.e., open ocean seawater) since Mo is almost entirely transferred to the sediments [*Neubert et al.*, 2008; *Nägler et al.*, 2011]. Net inflow of Mo through exchange of the basin water with open ocean seawater at a rate faster than the removal of Mo to sediments will lead to a euxinic basin with incomplete Mo drawdown [e.g., *Algeo and Lyons*, 2006], whose sediments are still fractionated by  $\sim -0.70\text{‰}$  from open ocean seawater [*Poulson et al.*, 2006] (as seen in modern Cariaco Basin [*Arnold et al.*, 2004]).

The only Mo-isotope study of mudrocks deposited during the T-OAE, undertaken on deposits from Yorkshire (Figures 1 and 2) [*Pearce et al.*, 2008], produced two key observations. First, the Mo-isotope composition of mudrocks deposited during the negative carbon-isotope excursion of the T-OAE (uppermost *semicelatum* Subzone of the *tenuicostatum* Zone and lower *exaratum* Subzone of the *falciferum* Zone) were interpreted to record a global seawater value that was lower than that of present-day seawater. This difference was interpreted by *Pearce et al.* [2008] to record a significantly greater global removal flux of Mo into sulphide-rich sediments during the T-OAE (and thus a larger area of seafloor covered by euxinic water masses). Second, the Mo-isotope compositions of the organic-rich mudrocks oscillated with an amplitude of  $\sim 0.70\text{‰}$  during the interval of the negative carbon-isotope excursion. Given the assumption by *Pearce et al.* [2008] of constant euxinia and quantitative Mo drawdown in the Cleveland Basin, and a similarity in timing to astronomically forced carbon cycle changes recorded by carbon isotopes in the same section [*Kemp et al.*, 2005], these Mo-isotope variations were interpreted to record temporal fluctuations in the removal of Mo into

oxic and sulphidic sediments at a global scale, possibly in response to episodes of methane hydrate dissociation and oxidation [Pearce *et al.*, 2008].

This study further investigates the use of Mo isotopes to constrain global- and local-scale redox changes during the T-OAE. Three new Mo-isotope profiles are presented (Figure 1): from the Dotternhausen Quarry section (South German Basin, Germany), from the Rijswijk core (West Netherlands Basin, Netherlands) and from the Dogna core (Belluno Basin, Southern Alps, northern Italy). Together with the published Yorkshire data of Pearce *et al.* [2008], these locations form a transect from the northwest European shelf to the Tethyan continental margin and contain coeval organic-rich mudrocks deposited in restricted intrashelf marine basins and in an open-marine pelagic setting.

## 2. Site Descriptions

The stratigraphy of the carbonate-rich shales and limestones exposed in the Dotternhausen Quarry section, SW Germany, is well established through existing ammonite biostratigraphy [Riegraf *et al.*, 1984], and carbon-isotope chemostratigraphy [Schouten *et al.*, 2000; Röhl *et al.*, 2001; Berner *et al.*, 2013; Suan *et al.*, 2015; this study].

The Rijswijk research core is composed of a succession of silty organic-rich mudrocks, from which the Posidonia Shale (Posidonienschiefer) was identified using gamma ray core logs. The chemostratigraphy of the core was further refined with organic carbon-isotope measurements of powdered samples obtained across the Posidonia Shale interval. Characteristic inflections of the carbon-isotope record can be used to tentatively assign ammonite-equivalent zones [cf. Jenkyns *et al.*, 2001]. However, at the base and top of the studied succession such assignments have not been made because of a lack of characteristic features in the carbon-isotope data.

No direct ammonite biostratigraphy exists for the pelagic limestones and interbedded manganoan carbonates and marls in the Dogna core, north Italy (Igne Formation), but ammonites found in exposed, stratigraphically equivalent sections nearby [Jenkyns *et al.*, 1985] establish a *falciferum* to *bifrons* Zone age for the pelagic limestones immediately overlying the interbedded black shales and manganoan limestones [Jenkyns *et al.*, 1985; Bellanca *et al.*, 1999]. Furthermore, the identification of a negative carbon-isotope excursion in the black-shale-limestone facies in the core itself dates the organic-rich interval as age equivalent to the lower *falciferum* Zone of northern Europe [Jenkyns *et al.*, 2001]. Sample placements were guided by the published high-resolution carbon-isotope stratigraphy of Jenkyns *et al.* [2001].

## 3. Methods

Samples from Dotternhausen were obtained from a freshly exposed quarry section as detailed by Gill *et al.* [2011], while samples from the Dogna and Rijswijk successions were sampled directly from the cores. All material was subsampled to remove exterior surfaces and crushed to a fine powder in an agate pestle and mortar. Sample aliquots from Dotternhausen were decarbonated in 2 M HCl and analyzed for total organic carbon (TOC) and organic-carbon isotopes using an Isotope Cube elemental analyzer connected to an Isoprime 100 isotope ratio mass spectrometer in the Department of Geosciences at Virginia Tech. Data were corrected to the Vienna Pee Dee belemnite scale by comparison to certified (IAEA CH-6 and IAEA CH-7) and commercial (Elemental Microanalysis wheat flour, sorghum flour, low organic soil, and urea) standards. Long-term reproducibility was estimated from analyses of these standards and replicate samples as  $\pm 0.10\text{‰}$  (1 standard deviation (SD)). TOC values for Dotternhausen samples were obtained as part of the isotopic analysis using commercial elemental standards. TOC values for the Rijswijk and Dogna cores were determined from  $\sim 50$  mg sample aliquots by Rock-Eval pyrolysis at the University of Oxford.

Mo isotopes were measured by digesting powdered sample aliquots in a mixture of 3:1 HNO<sub>3</sub>:HCl, following the addition of an isotopic spike solution enriched in <sup>100</sup>Mo and <sup>97</sup>Mo. Mo was purified from the rock matrix using anion-exchange chromatography [Dickson *et al.*, 2016] and measured in 80 ppb (spike plus sample) solutions on a Nu-Plasma MC-ICP-MS attached to a desolvating nebulizer. Sample beam intensities were monitored using 80 times integrations of 10 s each. Data were reprocessed off-line to obtain isotopic compositions, which are expressed as  $\delta^{98/95}\text{Mo}$  relative to a zero delta of NIST 3134 + 0.25 [Goldberg *et al.*, 2013;

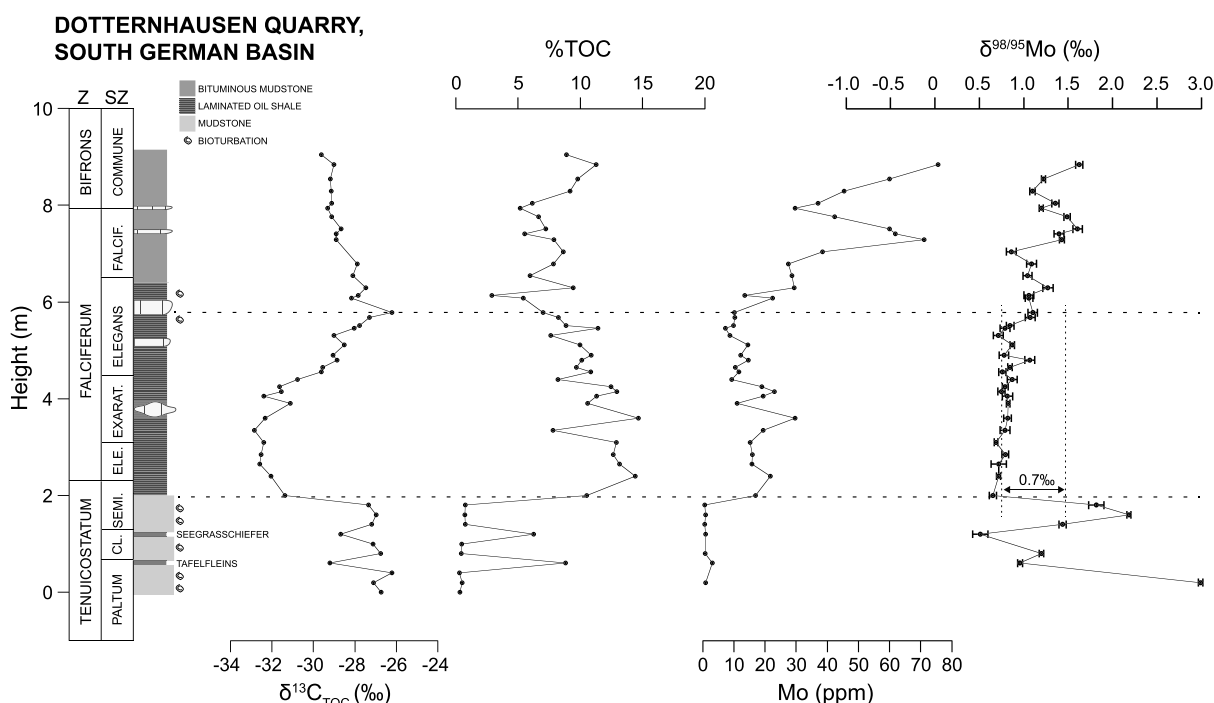


**Figure 3.** Geochemical data from Dotternhausen quarry, Germany. Ammonite stratigraphy is from Riegraf *et al.* [1984]. Vertical dashed lines highlight the range of the Mo-isotope fluctuations observed in the lower *falciferum* Zone in Yorkshire (as in Figure 2). Ele.: *elegantulum* Subzone. Note that the German ammonite scheme splits the *falciferum* Zone into four Subzones, compared to two Subzones in the English scheme [e.g., McArthur *et al.*, 2000].

Näglér *et al.*, 2014].  $\delta^{98/95}\text{Mo}$  data from Yorkshire [Pearce *et al.*, 2008] were previously published relative to an in-house standard ("Open University Mo") and have been recast here relative to NIST 3134 using a systematic correction of  $-0.12\text{‰}$  [Goldberg *et al.*, 2013]. Thirty digestions of the USGS SDO-1 shale standard gave an average value of  $1.04 \pm 0.08\text{‰}$  (2 SD), which is within uncertainty of the composition of  $1.05\text{‰}$  quoted by Goldberg *et al.* [2013]. Mo concentrations were calculated by isotope dilution from the same signal data used for isotopes, using the  $^{100}\text{Mo}/^{95}\text{Mo}$  ratio.

#### 4. Results

At Dotternhausen (Figure 3 and Table 1), Mo concentrations increase from the *semicelatum* Subzone of the *tenuicostatum* Zone into the stratigraphic interval of the negative carbon-isotope excursion of the T-OAE (*elegantulum*, *exaratum*, and *elegans* Subzones of the *falciferum* Zone in the German scheme, together equivalent to the *exaratum* Subzone in the English scheme), where Mo averages  $\sim 15$  ppm. Subsequently, Mo concentrations increase in the upper *falciferum* and *bifrons* Zones, where concentrations average  $\sim 50$  ppm, with two maxima of  $\sim 70$ – $75$  ppm. In the Rijswijk core (Figure 4), data coverage is low below the negative carbon-isotope excursion interval of the T-OAE. Mo concentrations vary in a similar manner to those at Dotternhausen, with an interval of low concentrations averaging 9 ppm during the negative carbon-isotope excursion interval, rising sharply to a maximum of 69 ppm in the interval stratigraphically equivalent to the lower *falciferum* Subzone. The stratigraphic trends in Mo concentrations at both locations are similar to the Yorkshire profile [Pearce *et al.*, 2008] (Figure 2), but absolute concentrations of Mo are highest at Dotternhausen. In contrast to Dotternhausen, Rijswijk, and Yorkshire, Mo concentrations in the Dogna core (Figure 5 and Table 2) increase only during the interval of the negative carbon-isotope excursion to an average of  $\sim 6$  ppm. At the top of this interval (equivalent to the upper *exaratum* Subzone of the English scheme), concentrations return to very low values ( $<1$  ppm) rather than increasing further as they do at Dotternhausen, Rijswijk, and Yorkshire. The different enrichments in Mo at each of the locations is reflected in the TOC concentrations: at Dogna, the interval equivalent to the lower *falciferum* Zone averages only  $\sim 2\%$ , whereas average concentrations in the same stratigraphic level at Dotternhausen and Rijswijk are both  $11\%$ , compared to  $8\%$  at Yorkshire [Jenkyns and Clayton, 1997; Schouten *et al.*, 2000; Röhl *et al.*, 2001; Frimmel *et al.*,

**Table 1.** Dotternhausen Geochemical Data

Sample	Section Height (cm)	$\delta^{13}\text{C}_{\text{org}}$	%TOC	Mo (ppm)	$\delta^{98/95}\text{Mo}$	2 SE Uncertainty
DO-1	0.00	-26.73	0.34			
DO-2	20.00	-27.12	0.52	0.89	2.99	0.02
DO-3	40.00	-26.23	0.31			
DO-4	60.00	-29.19	8.81	3.09	0.96	0.03
DO-5	80.00	-26.77	0.44	0.82	1.20	0.03
DO-6	100.00	-27.13	0.50			
DO-7	120.00	-28.70	6.25	0.98	0.51	0.08
DO-8	140.00	-27.19	0.77	0.62	1.44	0.04
DO-9	160.00	-26.96	0.74	0.97	2.19	0.02
DO-10	180.00	-27.34	0.78	0.62	1.82	0.08
DO-11	200.00	-31.38	10.53	16.95	0.65	0.04
DO-12	240.00	-32.04	14.43	21.67	0.72	0.02
DO-13	265.00	-32.60	13.16	15.83	0.72	0.08
DO-14	285.00	-32.52	12.64	15.96	0.79	0.04
DO-15	310.00	-32.39	12.90	15.27	0.69	0.02
DO-16	335.00	-32.85	7.82	19.36	0.79	0.06
DO-17	360.00	-32.32	14.66	29.67	0.82	0.04
DO-18	390.00	-31.11	10.61	11.10	0.82	0.02
DO-19	405.00	-32.40	11.33	19.49	0.82	0.06
DO-20	415.00	-31.53	12.95	23.05	0.75	0.04
DO-21	425.00	-31.63	12.48	19.08	0.79	0.03
DO-22	440.00	-30.78	8.22	9.36	0.87	0.06
DO-23	455.00	-29.63	10.83	11.67	0.76	0.04
DO-24	465.00	-29.55	9.70	10.44	0.85	0.02
DO-25	480.00	-28.85	10.13	14.59	1.07	0.06
DO-26	490.00	-29.06	10.89	12.18	0.78	0.05
DO-27	511.00	-28.51	9.98	14.56	0.87	0.03
DO-28	531.00	-29.01	7.64	8.73	0.71	0.06
DO-29	546.00	-28.03	11.42	7.33	0.79	0.05
DO-30	551.00	-27.78	8.85	9.93	0.85	0.04
DO-31	568.00	-27.31	8.26	10.31	1.07	0.06
DO-32	578.00	-26.22	7.03	10.18	1.10	0.05
DO-33	608.00	-28.17	5.45	22.50	1.06	0.04
DO-34	614.00	-27.84	2.91	13.52	1.06	0.06
DO-35	629.00	-27.46	9.44	29.35	1.27	0.06
DO-36	654.00	-28.09	5.97	28.59	1.04	0.05
DO-37	679.00	-27.88	7.85	27.50	1.09	0.06
DO-38	704.00		8.66	38.50	0.86	0.05
DO-39	729.00	-28.90	7.89	71.09	1.43	0.03
DO-40	741.00	-28.91	5.54	61.83	1.40	0.06
DO-41	751.00	-28.67	7.25	59.98	1.61	0.05
DO-42	776.00	-29.12	6.68	42.36	1.49	0.03
DO-43	794.00	-29.31	5.19	29.70	1.20	0.02
DO-44	804.00	-29.12	6.15	37.00	1.36	0.04
DO-45	829.00	-29.15	9.19	45.39	1.10	0.03
DO-46	854.00	-29.19	9.81	59.94	1.22	0.02
DO-47	884.00	-29.02	11.28	75.64	1.62	0.04
DO-48	904.00	-29.61	8.90			

2004; Cohen *et al.*, 2004; Kemp *et al.*, 2005, 2011; Pearce *et al.*, 2008; McArthur *et al.*, 2008]. Mo/TOC ratios, which have been suggested to reflect the inventory of dissolved Mo in euxinic marine basins [Algeo and Lyons, 2006], reach similar minimum values of  $\sim 1$  during the negative carbon-isotope excursion interval for Dotternhausen and Rijswijk, which are similar to those at Yorkshire in the equivalent stratigraphic interval [McArthur *et al.*, 2008]. More obvious differences in Mo/TOC ratios occur in samples from above the negative carbon-isotope excursion interval, where they span a range of  $\sim 1$ –10 at Dotternhausen and Rijswijk. This range is also very similar to the range of Mo/TOC values in Yorkshire in the equivalent strata [McArthur *et al.*, 2008].

At Dotternhausen (Figure 3),  $\delta^{98/95}\text{Mo}$  becomes as heavy as 2.99‰ in the upper *tenuicostatum* Zone but is lighter in two thin black-shale intervals (the Tafelfleins and the Seegrasschiefer), where  $\delta^{98/95}\text{Mo}$  is 0.96‰



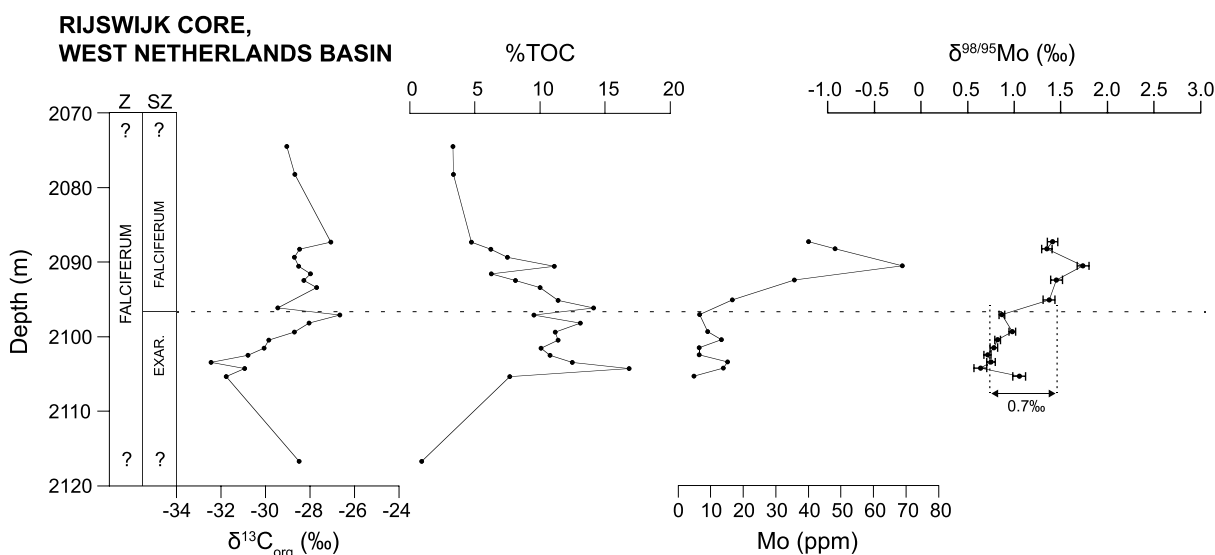


**Figure 4.** Geochemical data from the Rijswijk core, Netherlands. Ammonite zones are approximately inferred from the carbon-isotope chemostratigraphy. Vertical dashed lines highlight the range of the Mo-isotope fluctuations observed in the lower *falciform* Zone in Yorkshire (as in Figure 2).

and 0.51‰, respectively. Mo concentrations are also slightly enriched in these two shale units compared to the overlying and underlying samples, at ~1–3 ppm.  $\delta^{98/95}\text{Mo}$  shows little variation around an average of ~0.80‰ in the lower *falciform* Zone (*elegatulum*, *exaratum*, and the lower *elegans* Subzones) during the negative carbon-isotope excursion and then increases in two steps, first to an average of 1.07‰ halfway through the *elegans* Subzone and second to 1.38‰ in the *falciform* Subzone and *bifrons* Zone, respectively. The Rijswijk core (Figure 4) has a very similar pattern of  $\delta^{98/95}\text{Mo}$  to Dotternhausen, both in terms of stratigraphic trend and absolute values.  $\delta^{98/95}\text{Mo}$  averages 0.79‰ in the interval of the negative carbon-isotope excursion, before increasing in two steps, first to ~0.98‰ shortly before the inferred *exaratum-falciform* Subzone boundary, and second to ~1.40‰ in the inferred *falciform* Subzone (apart from a one-point maximum of 1.74‰). In the Dogna core,  $\delta^{98/95}\text{Mo}$  ranges from –1.39‰ to 0.68‰ and averages 0.19‰ in the interval of the negative carbon-isotope excursion (Figure 5).  $\delta^{98/95}\text{Mo}$  compositions

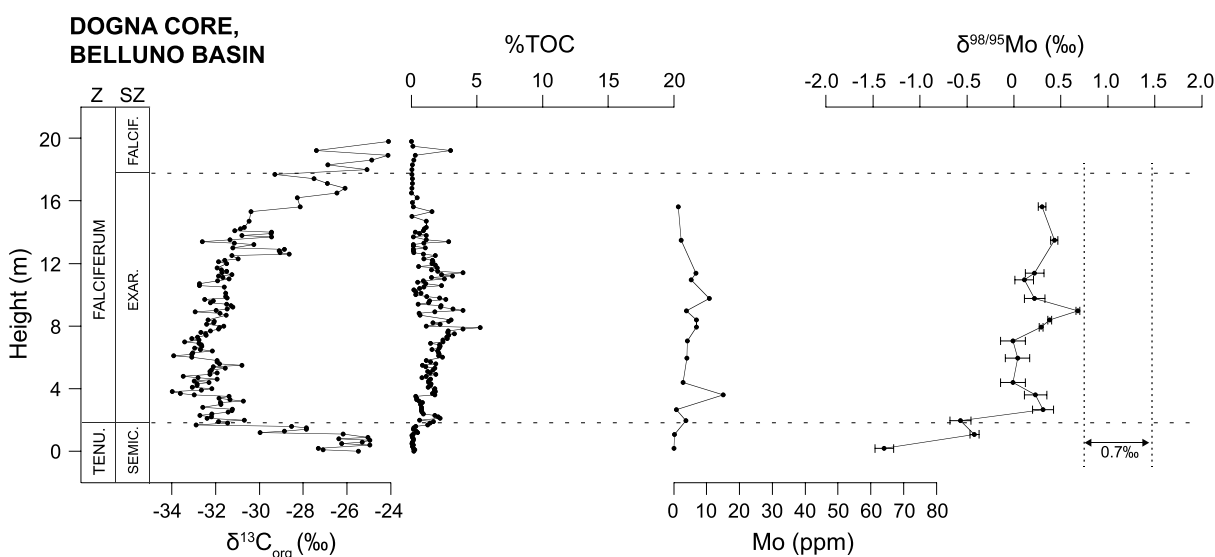


**Figure 5.** Geochemical data from the Dogna core, northern Italy. Ammonite zonation is inferred from the carbon-isotope data of *Jenkyns et al.* [2001], and from ammonite biostratigraphy of correlative outcrops described by *Jenkyns et al.* [1985]. TOC, Mo isotopes and concentrations are from this study. Vertical dashed lines highlight the range of the Mo-isotope fluctuations observed in the lower *falciform* Zone in Yorkshire (as in Figure 2).

**Table 2.** Rijswijk Core Geochemical Data

Depth	$\delta^{13}\text{C}_{\text{org}}$	TOC (%)	Mo (ppm)	$\delta^{98/95}\text{Mo}$	2 SE Uncertainty
2074.5	−29.04	3.32			
2078.23	−28.68	3.37			
2087.33	−27.07	4.76	40.00	1.41	0.06
2088.3	−28.46	6.24	48.20	1.35	0.06
2089.33	−28.70	7.52			
2090.55	−28.50	11.11	68.87	1.74	0.06
2091.55	−27.97	6.29			
2092.43	−28.27	8.11	35.67	1.45	0.06
2093.4	−27.70	10			
2095.1		11.4	16.65	1.37	0.06
2096.13	−29.45	14.12			
2097.13	−26.65	9.54	6.58	0.87	0.03
2098.15	−28.03	13.1			
2099.39	−28.69	11.18	9.04	0.98	0.03
2100.49	−29.85	11.4	13.36	0.82	0.03
2101.52	−30.06	10.09	6.44	0.78	0.04
2102.5	−30.78	10.8	6.45	0.71	0.04
2103.45	−32.44	12.48	15.16	0.75	0.04
2104.27	−30.94	16.84	13.87	0.64	0.07
2105.37	−31.77	7.69	4.93	1.06	0.07
2116.7	−28.49	0.92			

and Mo concentrations at Dogna are, therefore, always significantly lower than those observed at the more northerly locations.

## 5. Discussion

### 5.1. Mo-Isotope Systematics Prior to the T-OAE Negative Carbon-Isotope Excursion

At Yorkshire and Dotternhausen (Figures 2 and 3), the mudrocks deposited during the *tenuicostatum* Zone, prior to the negative carbon-isotope excursion interval, are characterized by bioturbated facies with low organic-carbon abundances (<1%), with a high proportion of terrestrially derived organic matter [Frimmel *et al.*, 2004; French *et al.*, 2014]. Benthic fauna was locally abundant and diverse in these deposits [Harries and Little, 1999; Caswell *et al.*, 2009; Caswell and Coe, 2013], which has been interpreted to reflect a relatively well-oxygenated environment that developed during a relative sea level highstand [Röhl *et al.*, 2001; Schmid-Röhl *et al.*, 2002; Frimmel *et al.*, 2004]. The pelagic limestones that underlie the black shale/marl interval in the Dogna core are also TOC-lean and characterized by high pristane/phytane ratios that record oxic depositional conditions [Farrimond *et al.*, 1994]. Consequently, the very light  $\delta^{98/95}\text{Mo}$  at Dogna below ~2 m can be related to the adsorption of Mo to sedimentary oxide minerals in sediments underlying an oxic water column, as observed in similar settings in the modern ocean [Siebert *et al.*, 2006; Poulson-Brucker *et al.*, 2009]. A similar interpretation has been made of the light Mo-isotope compositions of the *tenuicostatum*-Zone deposits in the Yorkshire succession [Pearce *et al.*, 2008]. At Dotternhausen, the heavier  $\delta^{98/95}\text{Mo}$  in the *tenuicostatum* Zone correspond to organic-lean deposits containing very low abundances of Mo and very low TOC. The two thin black-shale beds in this part of the succession, the Tafelfleins and the Seegrasschiefer, have previously been associated with short-lived anoxic conditions in the South German Basin [Röhl *et al.*, 2001; Frimmel *et al.*, 2004; Berner *et al.*, 2013; Montero-Serrano *et al.*, 2015] and notably contain slightly elevated Mo concentrations (1–3 ppm) and lower  $\delta^{98/95}\text{Mo}$  compared to the surrounding samples. The highly variable  $\delta^{98/95}\text{Mo}$  compositions from the *tenuicostatum* Zone can be hypothesized to reflect the mixing of authigenic Mo enrichments with lighter  $\delta^{98/95}\text{Mo}$  values (in the Tafelfleins and Seegrasschiefer), with nonauthigenic Mo phases with much heavier  $\delta^{98/95}\text{Mo}$  values.

### 5.2. Mo-Isotope Systematics During the T-OAE Negative Carbon-Isotope Excursion

The South German, West Netherlands, and Cleveland Basins were characterized by prolonged intervals of sulphidic conditions within the water column during the early Toarcian, as indicated by the elevated concentration of biomarkers for photosynthetic sulphide-oxidizing bacteria [Schouten *et al.*, 2000; Schwark and Frimmel,



2006; French *et al.*, 2014]; the near absence of benthic biota except for the local occurrence of the opportunistic pseudoplanktonic bivalve *Pseudomytiloides dubius* [Röhl *et al.*, 2001; Caswell *et al.*, 2009]; the absence of macroscale sedimentary bioturbation that would be associated with benthic organisms on the seafloor [Röhl *et al.*, 2001; Ghadeer and Macquaker, 2012]; and relatively elevated abundances of redox-sensitive trace metals [Brumsack, 1991; Pearce *et al.*, 2008; McArthur *et al.*, 2008; Montero-Serrano *et al.*, 2015; this study]. Such conditions have previously been used as evidence that the dissolved inventory of Mo within a basin may have been quantitatively drawn down within the basin itself, thus allowing the basin sediments to record a  $\delta^{98/95}\text{Mo}$  composition similar to open ocean seawater outside the basin [e.g., Arnold *et al.*, 2004; Gordon *et al.*, 2009; Dickson *et al.*, 2012]. However, euxinia cannot have been the only control on  $\delta^{98/95}\text{Mo}$  during this interval, because while the sediment  $\delta^{98/95}\text{Mo}$  values at Yorkshire periodically fluctuated between  $\sim 0.75\text{‰}$  and  $1.45\text{‰}$  during the T-OAE, sediment  $\delta^{98/95}\text{Mo}$  at Dotternhausen and Rijswijk varied much less around a value of  $\sim 0.80\text{‰}$  within the equivalent stratigraphic interval (Figures 2–4). Bearing in mind that authigenic phases in modern marine sediments do not record  $\delta^{98/95}\text{Mo}$  compositions higher than coeval seawater [Siebert *et al.*, 2003; Nögler *et al.*, 2011], this observation shows that when sediments in the Cleveland Basin evolved to higher  $\delta^{98/95}\text{Mo}$ , the coeval West Netherlands and South German Basin deposits must have been fractionated from the global seawater value. It would be difficult to explain the intersite differences in the sediment  $\delta^{98/95}\text{Mo}$  compositions of the Cleveland, West Netherlands, and South German Basins during the euxinic depositional conditions that prevailed during the T-OAE by invoking the mixing into sediments of isotopically light oxic molybdenum phases, because they would be unstable in such conditions. Rather, the sediment Mo at each location must have been dominated by Mo sulphides [Poulson-Brucker *et al.*, 2009, 2012; Neubert *et al.*, 2008; Nögler *et al.*, 2011], with a negligible mixing contribution from Mo adsorbed to oxyhydroxides. Consequently, evolution of the local seawater  $\delta^{98/95}\text{Mo}$  in each basin is most likely to have been the principal cause of the differences in the sedimentary isotope records. This situation differs from the  $\delta^{98/95}\text{Mo}$  of the Dogna deposits, where alternations between black shale and manganoan carbonate facies [Bellanca *et al.*, 1999] within the interval of the negative carbon-isotope excursion demonstrate that  $\delta^{98/95}\text{Mo}$  was probably affected by changes in Mo speciation under fluctuating bottom water redox conditions.

One possible explanation for differences in the evolution of local seawater  $\delta^{98/95}\text{Mo}$  in the South German, West Netherlands, and Cleveland Basins is that the periodic fluctuations in the Cleveland Basin sediment  $\delta^{98/95}\text{Mo}$  record the changing value of global seawater, due to global-scale changes in the removal fluxes of Mo into sulphidic and oxic sediments [Pearce *et al.*, 2008]. The absence of similar fluctuations in the West Netherlands and South German Basins must then have been due to fluctuations in redox and/or hydrographic state in those basins over this same interval.

There are several difficulties with this explanation. At Dotternhausen, there is no clear evidence for periodicity in basin-scale changes in oxygen ventilation during the interval of the negative carbon-isotope excursion. Small “event colonies” of the opportunistic bivalve *P. dubius* are scattered throughout the lower *falciferum* Zone and are thought to reflect brief episodes of basin oxygenation during storm events [Röhl *et al.*, 2001; Montero-Serrano *et al.*, 2015]. However, bivalves do not cluster in the three to four distinct intervals that would be expected if these short basinal reoxygenation events were occurring at the same time-scales of the Mo-isotope fluctuations in Yorkshire. Other changes observed in the basin also occur, but on timescales that do not match those for changes in  $\delta^{98/95}\text{Mo}$ .  $\text{C}_{13-17}/\text{C}_{18-22}$  aryl isoprenoid ratios, pristane/phytane ratios, and the presence of isorenieratene show that the influence of sulphidic water masses did not abate significantly until the mid-*elegans* Subzone (mid-*falciferum* Zone), when photic-zone euxinia became more episodic, and the chemocline moved deeper in the water column [Schouten *et al.*, 2000; Schwark and Frimmel, 2006]. A shift toward more intermittent euxinia during the *elegans* Subzone is also marked at Dotternhausen by the appearance of bioturbated horizons, indicating more prolonged recolonization of the seafloor by bivalves during episodes of seafloor reoxygenation. This event has been recognized in other South German Basin sections and therefore appears to have been a regional phenomenon [Röhl and Schmid-Röhl, 2004]. The geochemical and sedimentological data suggest that significant and prolonged oxygenation events in the South German Basin were restricted to the late *falciferum* Zone only. Biotic and sedimentological data are lacking for the Rijswijk core, but the similarity of Mo concentrations,  $\delta^{98/95}\text{Mo}$  compositions, and Mo/TOC ratios (Figure 6) imply that a similar situation could have prevailed in the West Netherlands Basin.

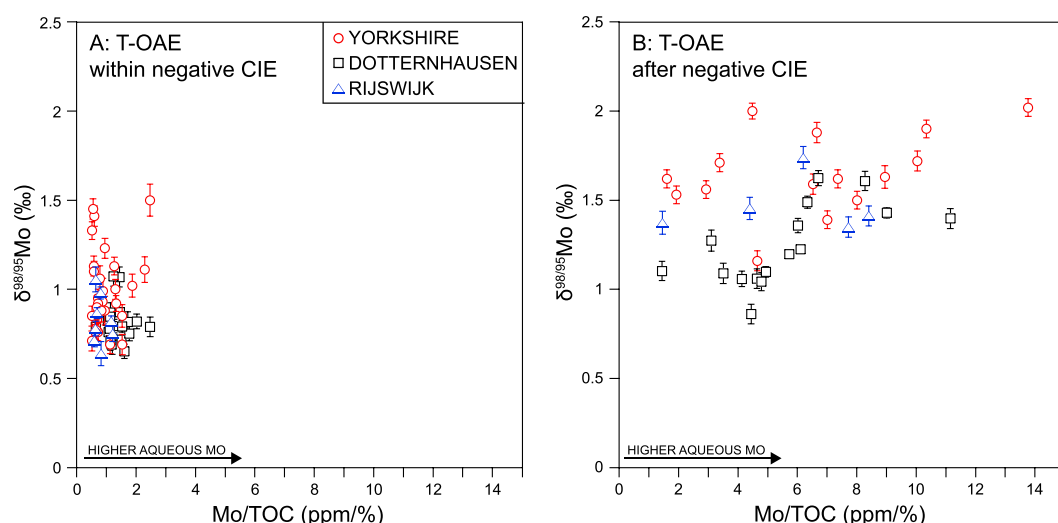


**Figure 6.** (a) Relationship between Mo/TOC ratios and  $\delta^{98/95}\text{Mo}$  of samples from within the negative carbon-isotope excursion interval and (b) postdating the negative carbon-isotope excursion interval (upper *falciferum* and *bifrons* ammonite Zones) in Yorkshire (black squares), Dotternhausen (red circles), and Rijswijk (green triangles). Horizontal dashed lines are the range of the Mo-isotope fluctuations found by Pearce et al. [2008] in Yorkshire. A larger inventory of Mo in global seawater affects geochemical species such as to give higher Mo/TOC and higher  $\delta^{98/95}\text{Mo}$  in Figure 6b.

By contrast, there is evidence for hydrographic instability at timescales similar to the fluctuations observed in  $\delta^{98/95}\text{Mo}$  in the Cleveland Basin. Caswell et al. [2009] and Caswell and Coe [2013] noted that the average size of *P. dubius* shells within the *falciferum* Zone varied within the same stratigraphic levels as the  $\delta^{98/95}\text{Mo}$  record of Pearce et al. [2008]. Mo concentrations also showed small increases (reflecting a higher availability of Mo in the basin seawater) at stratigraphic levels where  $\delta^{98/95}\text{Mo}$  becomes lighter (Figure 7). Taken together, the evidence for changing hydrographic conditions is inconsistent with the presence of the uniform hydrography in the Cleveland Basin that would be needed for deposits to continually record the global seawater  $\delta^{98/95}\text{Mo}$  values. Furthermore, the evidence for hydrographic changes in the West Netherlands and South German Basins is inconsistent with those that would be required to balance fluctuations in open ocean seawater  $\delta^{98/95}\text{Mo}$  and to maintain the relatively constant sediment Mo-isotope compositions observed at these locations.

A alternative explanation for the observed variations in  $\delta^{98/95}\text{Mo}$  in the Cleveland, West Netherlands, and South German Basins during the lower *falciferum* Zone ( $\sim 0.75\text{‰}$ ) is that extreme basin restriction prevailed at all three locations. This hydrographic configuration left the isotopic composition of basin waters to be dominated by Mo delivered by the weathering of catchment rocks [McArthur et al., 2008]. In this case, the periodic increases in sediment  $\delta^{98/95}\text{Mo}$  during the interval of the negative carbon-isotope excursion in Yorkshire, as well as the increases in  $\delta^{98/95}\text{Mo}$  from the *falciferum* Subzone and stratigraphically upward in Yorkshire, Rijswijk, and Dotternhausen, are explained by enhanced basin connectivity with the surrounding oceans. Such connectivity would increase the inventory of dissolved Mo in each basin; coeval increases to heavier  $\delta^{98/95}\text{Mo}$  in the accumulating sediments were then the result of mixing with open-ocean seawater with a  $\delta^{98/95}\text{Mo}$  of  $\sim 1.45\text{‰}$ , heavier than the local weathering fluxes.

However, there are also several observations that, when taken together, weigh against this explanation. First, the dominance of Mo derived from local weathering fluxes in each basin is inconsistent with the high similarity in sediment  $\delta^{98/95}\text{Mo}$  compositions ( $\sim 0.75\text{‰}$ ) found in the lower *falciferum* Zone equivalent deposits of the Rijswijk and Dotternhausen successions, and the lightest sediment  $\delta^{98/95}\text{Mo}$  in the equivalent interval in Yorkshire. Today, the isotopic composition of riverine Mo fluxes is controlled by the incongruent weathering of minerals from different rock types, and by the adsorption and desorption of Mo onto organic matter and oxyhydroxide minerals in river catchments [Pearce et al., 2010; Neubert et al., 2011; Siebert et al., 2016]. These processes result in a global range of  $\sim 2\text{‰}$  in modern river waters [Archer and Vance, 2008] and also at the scale of individual catchments draining similar rock types [Pearce et al., 2010; Neubert et al., 2011]. The near-identical  $\delta^{98/95}\text{Mo}$  values during the *falciferum* Zone-equivalent deposits in Yorkshire, Rijswijk,

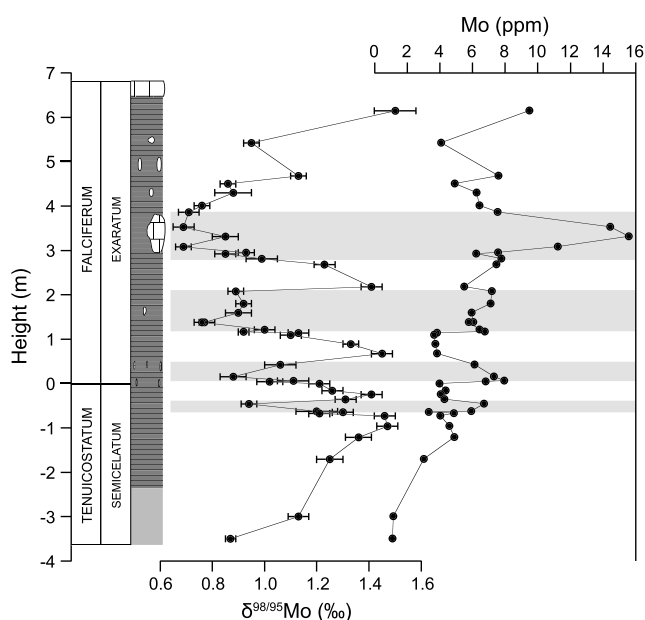


**Figure 7.** Relationship between  $\delta^{98/95}\text{Mo}$  and Mo concentrations of samples from the *semicelatum* and *exaratum* Subzones of the Yorkshire succession. Shaded bands highlight the inverse relationship between the two variables. This relationship is interpreted here to be due to fluctuations in the exchange rate of basin seawater with open ocean seawater. An enhanced rate of exchange would increase the local basin Mo inventory (higher Mo concentrations in the sediments) and inhibit quantitative removal of dissolved Mo into the basin sediments (lighter  $\delta^{98/95}\text{Mo}$ ). Data from Pearce *et al.* [2008].

and Dotternhausen are therefore more consistent with the presence of a water mass with a well-mixed Mo-isotope composition at all three locations than with the dominance of local Mo fluxes at the scale of each catchment.

Second, marine biomarkers are present throughout the *falciferum*-Zone deposits of the Yorkshire and Dotternhausen successions [Schouten *et al.*, 2000; French *et al.*, 2014]. The presence of marine biomarkers does not unambiguously point to a fully marine environment, because the timescale of biomarker production and burial is short compared to the very long timescales recorded by each rock succession [e.g., French *et al.*, 2014]. However, even very brief fully marine incursions would tend to dominate the local Mo inventory, given that the concentration of dissolved Mo in open ocean seawater would be at least an order of magnitude higher than in local rivers, even in a Toarcian world where global Mo concentrations may have been considerably less than present-day levels [e.g., Miller *et al.*, 2011].

Third, during the intervals when the marine Mo flux decreases sufficiently for the riverine Mo flux to dominate, the concentrations of Mo in the sediment are expected to substantially drop. This change is not observed in the data. Rather, the largest variations in Mo concentrations occur at Dotternhausen, where they are accompanied by insignificant variations in  $\delta^{98/95}\text{Mo}$ . In Yorkshire, increases in  $\delta^{98/95}\text{Mo}$  are actually accompanied by decreases in Mo concentrations, the opposite of what might be expected from a Mo inventory change influenced by enhanced mixing with open ocean seawater (Figure 7).

Lastly, in the highly stratified Cleveland Basin, riverine inputs may have generated a brackish surface water layer, and mixing of river-derived Mo into the basinal deep waters would have been severely inhibited. A good analogue of a basin in which this process occurs is the present-day Black Sea, where surface waters are dominated by riverine inputs, producing surface salinities of ~18 practical salinity units [Murray *et al.*, 1991]. Despite the significant riverine contributions to surface waters, and a > 90% drawdown of Mo in subchemocline waters, sediments accumulating below the chemocline at aqueous  $\text{H}_2\text{S}$  concentrations >11 mol/L have Mo-isotope compositions similar to that of open ocean seawater [Neubert *et al.*, 2008]. A stratified Cleveland Basin is supported by the abundance of gammacerane, a biomarker for stratification in ancient water bodies [Sinninghe Damsté *et al.*, 1995], which becomes more abundant in the *exaratum* Subzone of the Yorkshire Jet Rock compared to the underlying deposits of *tenuicostatum* Zone age [French *et al.*, 2014]. However,

gammacerane can also reflect seasonal stratification, so its relative abundance in the Jet Rock does not preclude occasional mixing events. Of course, since the paleodepth of the Cleveland Basin is not well constrained, the true hydrographic configuration cannot be unambiguously established. Nonetheless, if these conditions prevailed in the Cleveland Basin, it is hard to envisage how isotopically light Mo-isotope signatures in surface waters would come to dominate the sedimentary  $\delta^{98/95}\text{Mo}$  in the manner highlighted by McArthur *et al.* [2008].

A simpler explanation for the Mo-isotope data proposed here is that the global seawater Mo-isotope composition was constant during the lower *falciferum* Zone. In this situation, the variations observed at Yorkshire were governed by changes in the rate of open ocean seawater exchange into the Cleveland Basin. Periodic deviations to heavier  $\delta^{98/95}\text{Mo}$  in the Cleveland Basin are caused by a decreased rate of exchange, thus favoring a greater proportional removal of Mo from local seawater into the underlying sediments. This high removal efficiency would cause the basin sediments to evolve toward the composition of inflowing open ocean seawater. The constancy of the  $\delta^{98/95}\text{Mo}$  compositions of the Rijswijk and Dotternhausen successions (which are similar to the lightest values in the *exaratum* Subzone in Yorkshire) implies that the rate of seawater exchange with the open ocean was too rapid to enable substantial drawdown of aqueous Mo in those two basins (despite prevailing euxinia), similar to the present-day Cariaco Basin [Arnold *et al.*, 2004]. This explanation is strongly supported by the antiphase relationship between  $\delta^{98/95}\text{Mo}$  and Mo concentrations in the Yorkshire succession, which would be consistent with a decreased inventory of Mo in the basin (lower Mo concentrations) at times of enhanced drawdown into sediments (heavier  $\delta^{98/95}\text{Mo}$ ) (Figure 7).

In summary, although the Cleveland Basin was, in general, a sulphidic, restricted marine basin with a very low inventory of dissolved Mo, the renewal rate of the basin waters probably fluctuated over stratigraphic intervals in tune with the  $\delta^{98/95}\text{Mo}$  fluctuations. This argument implies that the Mo-isotope fluctuations at Yorkshire were not driven directly by changes in the burial of Mo into different redox environments at a global scale during the T-OAE [Pearce *et al.*, 2008], but rather by periodic changes in the hydrography and redox state of the Cleveland Basin. The broadly constant sediment  $\delta^{98/95}\text{Mo}$  in the South German Basin presumably occurred because the rate of seawater renewal was sufficient to limit the extent of water column Mo depletion, thus preserving a constant fractionation of Mo sulphides from overlying basin seawater. A similar situation appears to have prevailed in the West Netherlands Basin, although the comparatively low-resolution data set leaves open the possibility that it might also have been affected by brief increases in  $\delta^{98/95}\text{Mo}$  that are presently undetected.

At Dogna, the sediment  $\delta^{98/95}\text{Mo}$  compositions of  $-1.39\text{‰}$  to  $-0.65\text{‰}$  during the *falciferum* Zone-equivalent negative carbon-isotope excursion interval are heavier than the  $-1.55\text{‰}$  that would reflect the  $-3\text{‰}$  fractionation of Mo bound to manganese-oxyhydroxides from a seawater composition of  $-1.45\text{‰}$ , but lighter than the sediment compositions observed in the northerly euxinic basins. These values must therefore reflect the mixing of Mo bound to sulphides formed in pore waters and/or the water column [e.g., Poulson *et al.*, 2006; Scheiderich *et al.*, 2010] with Mo adsorbed to oxyhydroxide minerals [e.g., Siebert *et al.*, 2003; Barling and Anbar, 2004; Goldberg *et al.*, 2009]. This interpretation is consistent with the rather subtle oxygen depletion recorded during the T-OAE by pristane/phytane ratios and by the distribution of  $\text{C}_{27}$  and  $\text{C}_{29}$   $17\alpha$  hopanes and  $\text{C}_{33}$ – $\text{C}_{36}$  hopanes in this core [Farrimond *et al.*, 1994], and the repeated occurrence of manganoan limestones interbedded with black shales. These data indicate that the pelagic setting of the Belluno Basin would have inhibited the formation of water column  $\text{H}_2\text{S}$  as a result of the rapid renewal of bottom waters, as well as supporting the formation of authigenic oxyhydroxide minerals at the sediment-water interface [cf. Poulson *et al.*, 2006; Siebert *et al.*, 2006].

### 5.3. Mo-Isotope Systematics After the T-OAE Carbon-Isotope Excursion

The sediment  $\delta^{98/95}\text{Mo}$  values and Mo concentrations at Dotternhausen, Rijswijk, and Yorkshire increase within dark shale deposits above the lower *falciferum* Zone. A gradual increase in the abundance and diversity of benthic fauna in these deposits and a change from distinct to indistinct lamination [Röhl *et al.*, 2001; Schmid-Röhl *et al.*, 2002; Frimmel *et al.*, 2004] imply a slight increase in the oxygenation state of the three locations compared with the situation during the early *falciferum* Zone. Such basin-scale changes in redox would reduce the burial flux of Mo by inhibiting tetrathiomolybdate formation. A change in redox state would also cause a decrease in the sediment Mo-isotope composition by allowing the periodic delivery of isotopically

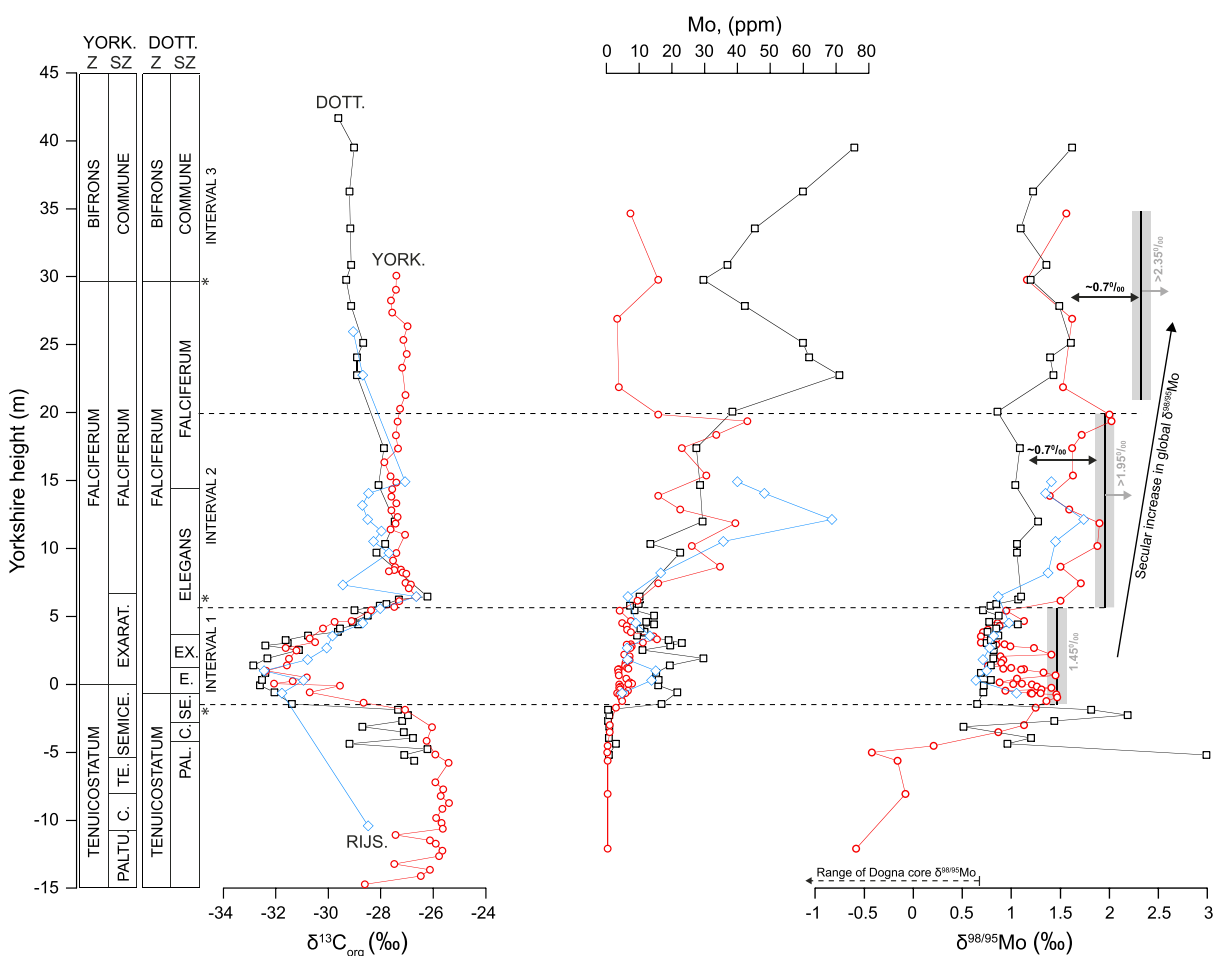


**Figure 8.** Inferred secular change in open ocean seawater  $\delta^{98/95}\text{Mo}$  over the T-OAE. The Dotternhausen data (open black circles: this study) have been rescaled to the vertical scale of the Yorkshshire data (open red circles [Cohen *et al.*, 2004; Kemp *et al.*, 2005; Pearce *et al.*, 2008]) by linearly interpolating between tie-points, marked with asterisks. These tie points are the *falciferum/bifrons* Zone boundary, and the base and top of the negative  $\delta^{13}\text{C}_{\text{org}}$  excursions in bulk organic matter recorded at each location. Inferred open ocean seawater  $\delta^{98/95}\text{Mo}$  values are marked for three intervals (marked 1–3 and discussed in the text) by a grey vertical bar, reflecting a  $\pm 0.10\text{‰}$  uncertainty. Arrows next to the vertical bars in intervals 2 and 3 highlight that these estimates of seawater  $\delta^{98/95}\text{Mo}$  are likely to be minimum values.

light Mo associated with oxyhydroxides to the sediments. The increases in Mo concentrations and  $\delta^{98/95}\text{Mo}$  can be explained by a global decrease in the removal of Mo from seawater into sulphidic sediments during waning of the T-OAE. This process would simultaneously increase the abundance and isotopic composition of Mo in seawater, overprinting any local changes in Mo speciation. Slight differences in the isotopic composition of coeval stratigraphic intervals above the negative carbon-isotope excursion interval, within the *falciferum* Zone, (Figures 6 and 8) can be attributed to differences in the evolving redox state of each basin (see section 5.2).

#### 5.4. Secular Trends in Global Ocean Oxygenation Across the T-OAE

The new multisite comparison of  $\delta^{98/95}\text{Mo}$  data through the lower Toarcian can be used to place approximate constraints on the evolution of global ocean oxygenation during the T-OAE. For the peak of the OAE itself (interval 1, Figure 8), the seawater Mo-isotope composition can be estimated to be close to the highest sediment  $\delta^{98/95}\text{Mo}$  registered at Yorkshshire:  $\sim 1.45\text{‰}$ . This value is significantly lower than the present-day seawater composition of  $2.34\text{‰}$  [Nakagawa *et al.*, 2012], implying a greater flux of Mo into sulphidic marine sediments during the T-OAE.

Following the negative carbon-isotope excursion interval of the T-OAE, the increase in  $\delta^{98/95}\text{Mo}$  and Mo concentrations at three locations (Figures 6 and 8) is consistent with a decrease in the global burial flux of

**Table 3.** Dogna Geochemical Data

Core Depth (m)	TOC (%)	Mo (ppm)	$\delta^{98/95}\text{Mo}$	2 SE Uncertainty
15.63	2.05	1.42	0.30	0.04
13.47	1.58	2.28	0.43	0.04
11.38	3.21	6.79	0.22	0.10
10.94	2.94	5.29	0.11	0.10
9.75	0.9	10.80	0.22	0.11
8.97	2.63	3.78	0.68	0.02
8.38	3.01	6.89	0.38	0.02
7.92	3.34	6.88	0.29	0.02
7.05	2.34	4.13	-0.01	0.13
5.95	2.03	3.94	0.04	0.13
4.38	1.13	2.83	-0.01	0.13
3.59	1.67	15.09	0.23	0.12
2.66	0.31	0.83	0.31	0.11
1.96	1.98	3.68	-0.57	0.11
1.08	0.19	0.18	-0.42	0.05
0.18	0.11	0.11	-1.38	0.10

Mo sulphides, thus indicating a contraction in the worldwide extent of seafloor euxinia. Placing bounds on the magnitude of the secular seawater Mo-isotope increase is not, however, straightforward, because of the potential for changes in the speciation of authigenic Mo in the deposits at Yorkshire, Dotternhausen, and Rijswijk. The high Mo concentrations occurring in the slightly bioturbated mudrock facies that characterize these successions suggests that an analogy may be drawn with sediments accumulating in present-day depositional systems where sulphidic sediments underlie oxic or suboxic seawater. In these locations today, Mo is enriched within sulphidic sediments but is isotopically lighter by  $\sim 0.7\text{‰}$  compared to the overlying seawater [e.g., Poulson *et al.*, 2006; Siebert *et al.*, 2006]. By analogy, therefore, the seawater Mo-isotope composition from the upper *falciferum* Zone upwards (interval 3, Figure 8) may reasonably be considered to have been greater than  $\sim 2.35\text{‰}$  (i.e.,  $\sim 0.7\text{‰}$  heavier than the sediment  $\delta^{98/95}\text{Mo}$ ).

For interval 2 (Figure 8), the fact that the intersite difference in  $\delta^{98/95}\text{Mo}$  between Yorkshire and Dotternhausen is  $\sim 0.70\text{‰}$  suggests that  $\sim 1.95\text{‰}$  can be adopted as a lower limit on the open ocean seawater Mo-isotope composition. Even if precise quantification is difficult, the data establish that there was a clear secular trend towards a reduction in the global burial flux of Mo sulphides following the T-OAE, and a concurrent increase in global oxygenation (Figure 8). A secular trend toward less extensive global anoxia following the T-OAE is recorded at many individual locations worldwide by a decrease in organic matter content, and by changes in sedimentary facies that reflect better oxygenation of the seafloor [e.g., Jenkyns *et al.*, 1985; Jenkyns, 1988]. Indeed, in exposures close to Dogna, the interval equivalent to the *bifrons* Zone, which overlies the interbedded organic-rich shales and manganoan limestones, is represented by nodular red limestones of rosso ammonitico facies [Jenkyns *et al.*, 1985; Bellanca *et al.*, 1999].

## 6. Conclusions

New Mo-isotope data have been presented from three locations (Rijswijk, West Netherlands Basin, Netherlands; Dotternhausen, South German Basin, Germany; and Dogna, Belluno Basin, northern Italy) spanning the northwest European epicontinental shelf and Tethyan continental margin, which reflect differing paleodepositional regimes during the early Toarcian. A detailed comparison of the new data with an existing Mo-isotope record from Yorkshire (Cleveland Basin, UK) [Pearce *et al.*, 2008] allows some key conclusions to be reached:

1. The global seawater  $\delta^{98/95}\text{Mo}$  for the interval of the negative carbon-isotope excursion of the T-OAE was close to  $1.45\text{‰}$ , substantially lower than the present-day value ( $\sim 2.34\text{‰}$ ).
2. A new explanation for fluctuations in sediment  $\delta^{98/95}\text{Mo}$  observed during the negative carbon-isotope excursion interval of the T-OAE in Yorkshire is presented. Previous explanations invoking expansions and contractions of seafloor euxinia at a global scale during the T-OAE, and the dominance of weathering fluxes of Mo to the Cleveland Basin, are inconsistent with the multisite data presented here. Instead, variations in sediment  $\delta^{98/95}\text{Mo}$  values for this interval are more likely to have been caused by



fluctuations in the exchange rate of open ocean seawater with Cleveland Basin water, which altered the amount of aqueous Mo depletion. The absence of similar fluctuations in sediment  $\delta^{98/95}\text{Mo}$  at sites located in the West Netherlands and South German Basins implies that although these areas were euxinic during the T-OAE, the local seawater exchange rate was sufficient to inhibit substantial drawdown of Mo by removal to the basin sediments.

3. The multisite data are consistent with a secular shift in seawater  $\delta^{98/95}\text{Mo}$  from  $\sim 1.45\text{‰}$  to  $>2.35\text{‰}$  between the negative carbon-isotope excursion interval of the T-OAE and the late *falciferum* Zone/early *bifrons* Zone. This trend is diagnostic of a global shift toward less extensive seafloor euxinia in the latter stages of the T-OAE. This phenomenon is recorded in the more hydrographically exposed pelagic Belluno Basin (Dogna core and associated outcrops) by the switch from interbedded manganoan carbonates and laminated black shales to grey and red pelagic limestones that are effectively devoid of organic matter.
4. Subtle differences in the Mo-isotope composition of deposits formed in different euxinic subbasins of the European epicontinental shelf were probably governed by local variations in basin hydrography and the rate at which basin waters were exchanged with open ocean waters.

# Acknowledgments

This work was funded by Shell Global Solutions International B.V. and the National Science Foundation (EAR-0719911). Data are available in Tables 1–3 or on request from the corresponding author (alex.dickson@earth.ox.ac.uk). The authors wish to thank Guillaume Suan, an anonymous reviewer, and the Editor Heiko Pälke for constructive comments.

# References

- Algeo, T. J., and T. W. Lyons (2006), Mo–total organic carbon covariation in modern anoxic marine environments: Implications for analysis of paleoredox and paleohydrologic conditions, *Paleoceanography*, 21, PA1016, doi:10.1029/PA001112.
- Al-Suwaidi, A., G. N. Angelozzi, F. Baudin, S. E. Damborenea, S. P. Hesselbo, H. C. Jenkyns, M. O. Manceñido, and A. C. Riccardi (2010), First record of the early Toarcian Oceanic Anoxic Event from the Southern Hemisphere, Neuquén Basin, Argentina, *J. Geol. Soc.*, 167, 633–636.
- Al-Suwaidi, A. H., S. P. Hesselbo, S. E. Damborenea, M. O. Manceñido, H. C. Jenkyns, A. C. Riccardi, G. N. Angelozzi, and F. Baudin (2016), The Toarcian Oceanic Anoxic Event (Early Jurassic) in the Neuquén Basin, Argentina: A reassessment of age and carbon isotope stratigraphy, *J. Geol.*, 124, 171–193.
- Archer, C., and D. Vance (2008), The isotopic signature of the global riverine molybdenum flux and anoxia in the ancient oceans, *Nat. Geosci.*, 1, 597–600.
- Arnold, G. L., A. D. Anbar, J. Barling, and T. W. Lyons (2004), Molybdenum isotope evidence for widespread anoxia in mid-Proterozoic oceans, *Science*, 304, 87–90.
- Barling, J., and A. D. Anbar (2004), Molybdenum isotope fractionation during adsorption by manganese oxides, *Earth Planet. Sci. Lett.*, 217, 315–329.
- Bellanca, A., D. Masetti, R. Neri, and F. Venezia (1999), Geochemical and sedimentological evidence of productivity cycles recorded in Toarcian black shales from the Belluno Basin, southern Alps, northern Italy, *J. Sediment. Res.*, 69, 466–476.
- Berner, Z. A., H. Puchelt, T. Nöltner, and T. U. Kramar (2013), Pyrite geochemistry in the Toarcian Posidonia Shale of south-west Germany: Evidence for contrasting trace-element patterns of diagenetic and syngenetic pyrite, *Sedimentology*, 60, 548–573.
- Brumsack, H.-J. (1991), Inorganic geochemistry of the German “Posidonia Shale”: Palaeoenvironmental consequences, in *Modern and Ancient Continental Shelf Anoxia*, edited by R. V. Tyson and T. H. Pearson, *Geol. Soc. Spec. Publ.*, 58, 353–362.
- Caruthers, A. H., D. R. Gröcke, and P. L. Smith (2011), The significance of an Early Jurassic (Toarcian) carbon-isotope excursion in Haida Gwaii (Queen Charlotte Islands), British Columbia, Canada, *Earth Planet. Sci. Lett.*, 307, 19–26.
- Caswell, B. A., and A. L. Coe (2013), Primary productivity controls on opportunistic bivalves during Early Jurassic oceanic deoxygenation, *Geology*, 41, 1163–1166.
- Caswell, B. A., A. L. Coe, and A. S. Cohen (2009), New range data for marine invertebrate species across the early Toarcian (Early Jurassic) mass extinction, *J. Geol. Soc.*, 166, 859–872.
- Cohen, A. S., A. L. Coe, S. M. Harding, and L. Schwark (2004), Osmium isotope evidence for the regulation of atmospheric  $\text{CO}_2$  by continental weathering, *Geology*, 32, 157–160.
- Dickson, A. J., A. S. Cohen, and A. L. Coe (2012), Seawater oxygenation during the Paleocene-Eocene Thermal Maximum, *Geology*, 40, 639–642.
- Dickson, A. J., H. C. Jenkyns, D. Porcelli, S. van den Boorn, and E. Idiz (2016), Basin-scale controls on the molybdenum-isotope composition of seawater during Oceanic Anoxic vent 2 (late Cretaceous), *Geochim. Cosmochim. Acta*, 178, 291–306.
- Eriksson, B. E., and G. R. Helz (2000), Molybdenum (IV) speciation in sulphidic waters: Stability and lability of thiomolybdates, *Geochim. Cosmochim. Acta*, 64, 1149–1158.
- Farrimond, P., D. P. Stoddart, and H. C. Jenkyns (1994), An organic geochemical profile of the Toarcian anoxic event in northern Italy, *Chem. Geol.*, 111, 17–33.
- French, K. L., J. Sepúlveda, J. Trabucho-Alexandre, D. R. Gröcke, and R. E. Summons (2014), Organic geochemistry of the early Toarcian oceanic anoxic event in Hawsker Bottoms, Yorkshire, England, *Earth Planet. Sci. Lett.*, 390, 116–127.
- Frimmel, A., W. Oschmann, and L. Schwark (2004), Chemostratigraphy of the Posidonia Black Shale, SW Germany I: Influence of sea-level variation on organic facies evolution, *Chem. Geol.*, 206, 199–230.
- Fu, X., J. Wang, X. Feng, D. Wang, W. Chen, C. Song, and S. Zeng (2016), Early Jurassic carbon-isotope excursion in the Qiangtang Basin (Tibet), the eastern Tethys: Implications for the Toarcian oceanic anoxic event, *Chem. Geol.*, 442, 62–72.
- Ghadeer, S. G., and J. H. S. Macquaker (2012), The role of event beds in the preservation of organic carbon in fine-grained sediments: Analyses of the sedimentological processes operating during deposition of the Whitby Mudstone Formation (Toarcian, Lower Jurassic) preserved in northeast England, *Mar. Pet. Geol.*, 35, 309–320.
- Gill, B. C., T. W. Lyons, and H. C. Jenkyns (2011), A global perturbation to the sulfur cycle during the Toarcian Oceanic Anoxic Event, *Earth Planet. Sci. Lett.*, 312, 484–496.
- Goldberg, T., C. Archer, D. Vance, and S. W. Poulton (2009), Mo isotope fractionation during adsorption to Fe (oxyhydr)oxides, *Geochim. Cosmochim. Acta*, 73, 6502–6516.
- Goldberg, T., G. Gordon, G. Izon, C. Archer, C. R. Pearce, J. McManus, A. D. Anbar, and M. Rehkämper (2013), Resolution of inter-laboratory discrepancies in Mo isotope data: An intercalibration, *J. Anal. At. Spectrom.*, 28, 724–735.

- Gordon, G. W., T. W. Lyons, G. L. Arnold, J. Roe, B. B. Sageman, and A. D. Anbar (2009), When do black shales tell molybdenum isotope tales?, *Geology*, **37**, 535–538.
- Gröcke, D. R., R. S. Hori, J. Trabucho-Alexandre, D. B. Kemp, and L. Schwark (2011), An open ocean record of the Toarcian oceanic anoxic event, *Solid Earth*, **2**, 245–257.
- Harries, P. J., and C. T. S. Little (1999), The Early Toarcian (Early Jurassic) and the Cenomanian–Turonian (Late Cretaceous) mass extinctions: Similarities and contrasts, *Palaeogeogr. Palaeoclimatol. Palaeoecol.*, **154**, 39–66.
- Helz, G. R., C. V. Miller, J. M. Charnock, J. F. W. Mosselmans, R. A. D. Patrick, C. D. Garner, and D. J. Vaughan (1996), Mechanism of molybdenum removal from the sea and its concentration in black shales: EXAFS evidence, *Geochim. Cosmochim. Acta*, **60**, 3631–3642.
- Hesselbo, S. P., D. R. Gröcke, H. C. Jenkyns, C. J. Bjerrum, P. Farrimond, H. S. Morgans Bell, and O. R. Green (2000), Massive dissociation of gas hydrate during a Jurassic oceanic anoxic event, *Nature*, **406**, 392–395.
- Hesselbo, S. P., H. C. Jenkyns, L. V. Duarte, and L. C. V. Oliveira (2007), Carbon-isotope record of the Early Jurassic (Toarcian) Oceanic Anoxic Event from fossil wood and marine carbonate (Lusitanian Basin, Portugal), *Earth Planet. Sci. Lett.*, **253**, 455–470.
- Howarth, M. K. (1973), The stratigraphy and ammonite fauna of the upper Liassic Grey Shales of the Yorkshire coast, *Bull. British Museum Nat. History Geol.*, **24**, 235–277.
- Howarth, M. K. (1992), The ammonite family Hiloceratidae in the lower Jurassic of Britain, *Palaeogr. Soc. Monogr.*, **145**, 1–200.
- Jenkyns, H. C. (1988), The early Toarcian (Jurassic) anoxic event: Stratigraphy, sedimentary and geochemical evidence, *Am. J. Sci.*, **288**, 101–151.
- Jenkyns, H. C. (2010), Geochemistry of oceanic anoxic events, *Geochem. Geophys. Geosyst.*, **11**, Q03004, doi:10.1029/2009GC002788.
- Jenkyns, H. C., and C. J. Clayton (1997), Lower Jurassic epicontinental carbonates and mudstones from England and Wales: Chemostratigraphic signals and the early Toarcian anoxic event, *Sedimentology*, **44**, 687–706.
- Jenkyns, H. C., M. Sarti, D. Masetti, and M. K. Howarth (1985), Ammonites and stratigraphy of Lower Jurassic black shales and pelagic limestones from the Belluno Trough, Southern Alps, Italy, *Eclogae Geol. Helv.*, **78**, 299–311.
- Jenkyns, H. C., D. R. Gröcke, and S. P. Hesselbo (2001), Nitrogen isotope evidence for water mass denitrification during the early Toarcian (Jurassic) oceanic anoxic event, *Paleoceanography*, **16**, 593–603, doi:10.1029/2000PA000558.
- Jenkyns, H. C., C. E. Jones, D. R. Gröcke, S. P. Hesselbo, and D. N. Parkinson (2002), Chemostratigraphy of the Jurassic System: Applications, limitations and implications for palaeoceanography, *J. Geol. Soc.*, **159**, 351–378.
- Kemp, D. B., and K. Izumi (2014), Multiproxy geochemical analysis of a Panthalassic margin record of the early Toarcian oceanic anoxic event (Toyora area, Japan), *Palaeogeogr. Palaeoclimatol. Palaeoecol.*, **414**, 332–341.
- Kemp, D. B., A. L. Coe, A. S. Cohen, and L. Schwark (2005), Astronomical pacing of methane release in the Early Jurassic period, *Nature*, **437**, 396–399.
- Kemp, D. B., A. L. Coe, A. S. Cohen, and G. P. Weedon (2011), Astronomical forcing and chronology of the early Toarcian (Early Jurassic) oceanic anoxic event in Yorkshire, UK, *Paleoceanography*, **26**, PA4210, doi:10.1029/2011PA002122.
- McArthur, J. M., D. T. Donovan, M. F. Thirlwall, B. W. Fouke, and D. Mathey (2000), Strontium isotope profile of the early Toarcian (Jurassic) oceanic anoxic event, the duration of ammonite biozones, and belemnite palaeotemperatures, *Earth Planet. Sci. Lett.*, **179**, 269–285.
- McArthur, J. M., T. J. Algeo, B. van de Schootbrugge, Q. Li, and R. J. Howarth (2008), Basinal restriction, black shales, Re-Os dating, and the Early Toarcian (Jurassic) oceanic anoxic event, *Paleoceanography*, **23**, PA4217, doi:10.1029/2008PA001607.
- McElwain, J. C., J. Wade-Murphy, and S. P. Hesselbo (2005), Changes in carbon dioxide during an oceanic anoxic event linked to intrusion into Gondwana coals, *Nature*, **435**, 479–482.
- Miller, C. A., B. Peucker-Ehrenbrink, B. D. Walker, and F. Marcantonio (2011), Re-assessing the surface cycling of molybdenum and rhenium, *Geochim. Cosmochim. Acta*, **75**, 7146–7179.
- Montero-Serrano, J. C., K. B. Föllmi, T. Adatte, J. E. Spangenberg, N. Tribouillard, A. Fantasia, and G. Suan (2015), Continental weathering and redox conditions during the early Toarcian Oceanic Anoxic Event in the northwestern Tethys: Insight from the Posidonia Shale section in the Swiss Jura mountains, *Palaeogeogr. Palaeoclimatol. Palaeoecol.*, **429**, 83–99.
- Murray, R. W., Z. Top, and E. Ozsoy (1991), Hydrographic properties and ventilation of the Black Sea, *Deep Sea Res., Part A*, **38**, 663–689.
- Näglér, T. F., N. Neubert, M. E. Böttcher, O. Dellwig, and B. Schnetger (2011), Molybdenum isotope fractionation in pelagic euxinia: Evidence from the modern Black and Baltic Seas, *Chem. Geol.*, **289**, 1–11.
- Näglér, T. F., A. D. Anbar, C. Archer, T. Goldberg, G. W. Gordon, N. D. Greber, C. Siebert, Y. Sohrin, and D. Vance (2014), Proposal for an international molybdenum isotope measurement standard and data representation, *Geostand. Geoanal. Res.*, **38**, 149–151.
- Nakagawa, Y., S. Takano, M. L. Firdaus, K. Norisuye, T. Hirata, D. Vance, and Y. Sohrin (2012), The molybdenum isotopic composition of the modern ocean, *Geochem. J.*, **46**, 131–141.
- Neubert, N., T. F. Näglér, and M. E. Böttcher (2008), Sulphidity controls molybdenum isotope fractionation into euxinic sediments: Evidence from the modern Black Sea, *Geology*, **36**, 775–778.
- Neubert, N., A. R. Heri, A. R. Voegelin, T. F. Näglér, F. Schlunegger, and I. M. Villa (2011), The molybdenum isotopic composition in river water: Constraints from small catchments, *Earth Planet. Sci. Lett.*, **304**, 180–190.
- Pálffy, J., and P. L. Smith (2000), Synchrony between Early Jurassic extinction, oceanic anoxic event, and the Karoo–Ferrar flood basalt volcanism, *Geology*, **28**, 747–750.
- Pearce, C. R., A. S. Cohen, A. L. Coe, and K. W. Burton (2008), Molybdenum isotope evidence for global ocean anoxia coupled with perturbations to the carbon cycle during the Early Jurassic, *Geology*, **36**, 231–234.
- Pearce, C. R., K. W. Burton, P. A. E. Pogge van Strandmann, R. H. James, and S. R. Gislason (2010), Molybdenum isotope behaviour accompanying weathering and riverine transport in a basaltic terrain, *Earth Planet. Sci. Lett.*, **295**, 104–114.
- Percival, L. M. E., M. L. I. Witt, T. A. Mather, M. Hermoso, H. C. Jenkyns, S. P. Hesselbo, A. Al-Suwaidi, M. S. Storm, W. Xu, and M. Ruhl (2015), Globally enhanced mercury deposition during the end-Pleinsbachian extinction and Toarcian OAE: A link to the Karoo–Ferrar Large Igneous Province, *Earth Planet. Sci. Lett.*, **428**, 267–280.
- Poulson, R. L., C. Siebert, J. McManus, and W. M. Berelson (2006), Authigenic molybdenum isotope signatures in marine sediments, *Geology*, **34**, 617–620.
- Poulson-Brucker, R. L., J. McManus, S. Severmann, and W. M. Berelson (2009), Molybdenum behavior during early diagenesis: Insights from Mo isotopes, *Geochem. Geophys. Geosyst.*, **10**, Q06010, doi:10.1029/2008GC002180.
- Poulson-Brucker, R. L., J. McManus, and S. W. Poulton (2012), Molybdenum isotope fractionations observed under anoxic experimental conditions, *Geochem. J.*, **46**, 201–209.
- Riegraf, W., G. Werner, and F. Lörcher (1984), *Der Posidonienschiefer—Biostratigraphie, Fauna und Fazies des südwestdeutschen Untertoarciums (Lias e)*, 195 pp., Enke, Stuttgart, Germany.

- Röhl, H.-J., and A. Schmid-Röhl (2004), Lower Toarcian (Upper Liassic) black shales of the central European epicontinental basin: A sequence stratigraphic case study from the SW German Posidonia Shale in *The Deposition of Organic-Carbon-Rich Sediments: Models, Mechanisms and Consequences*, *SEPM Spec. Publ.*, vol. 82, edited by N. B. Harris, pp. 165–189.
- Röhl, H.-J., A. Schmid-Röhl, W. Oschmann, A. Frimmel, and L. Schwark (2001), The Posidonia Shale (Lower Toarcian) of SW Germany: An oxygen-depleted ecosystem controlled by sea level and palaeoclimate, *Palaeogeogr. Palaeoclimatol. Palaeoecol.*, 169, 273–299.
- Scheiderich, K., G. R. Helz, and R. J. Walker (2010), Century-long record of Mo isotopic composition in sediments of a seasonally anoxic estuary (Chesapeake Bay), *Earth Planet. Sci. Lett.*, 289, 189–197.
- Schmid-Röhl, A., H.-J. Röhl, W. Oschmann, A. Frimmel, and L. Schwark (2002), Palaeoenvironmental reconstruction of Lower Toarcian epicontinental black shales (Posidonia Shale, SW Germany): Global versus regional control, *Geobios*, 35, 13–20.
- Schouten, S., H. M. E. van Kaam-Peters, W. I. C. Rijpstra, M. Schoell, and J. S. Sinninghe Damsté (2000), Effects of an oceanic anoxic event of the stable carbon isotopic composition of early Toarcian carbon, *Am. J. Sci.*, 300, 1–22.
- Schwark, L., and A. Frimmel (2006), Chemostratigraphy of the Posidonia Black Shale, SW Germany II: Assessment of extent and persistence of photic-zone anoxia using aryl isoprenoids distributions, *Chem. Geol.*, 206, 231–248.
- Siebert, C., T. F. Nägler, F. von Blanckenburg, and J. D. Kramers (2003), Molybdenum isotope records as a potential new proxy for paleoceanography, *Earth Planet. Sci. Lett.*, 211, 159–171.
- Siebert, C., J. McManus, A. Bice, R. Poulson, and W. M. Berelson (2006), Molybdenum isotope signatures in continental margin sediments, *Earth Planet. Sci. Lett.*, 241, 723–733.
- Siebert, C., J. C. Pett-Ridge, S. Opfergelt, R. A. Guicharnaud, A. N. Halliday, and K. W. Burton (2016), Molybdenum isotope fractionation in soils: Influence of redox conditions, organic matter, and atmospheric inputs, *Geochim. Cosmochim. Acta*, 162, 1–24.
- Sinninghe Damsté, J. S., F. Kenig, M. P. Koopmans, J. Köster, S. Schouten, J. M. Hayes, and J. W. de Leeuw (1995), Evidence for gammacerane as an indicator of water column stratification, *Geochim. Cosmochim. Acta*, 59, 1895–1900.
- Suan, G., et al. (2011), Polar record of Early Jurassic massive carbon injection, *Earth Planet. Sci. Lett.*, 312, 102–113.
- Suan, G., B. van de Schootbrugge, T. Adatte, J. Fiebig, and W. Oschmann (2015), Calibrating the magnitude of the Toarcian carbon cycle perturbation, *Paleoceanography*, 30, 495–509, doi:10.1002/2014PA002758.
- Svensen, H., S. Planke, L. Chevallier, A. Mørth-Sørensen, F. Corfu, and B. Jamveit (2007), Hydrothermal venting of greenhouse gases triggering Early Jurassic global warming, *Earth Planet. Sci. Lett.*, 256, 554–566.
- van der Schootbrugge, B., J. M. McArthur, T. R. Bailey, Y. Rosenthal, J. D. Wright, and K. G. Miller (2005), Toarcian oceanic anoxic event: An assessment of global causes using belemnite C isotope records, *Paleoceanography*, 20, PA3008, doi:10.1029/2004PA001102.
- Wasylenki, L. E., C. L. Weeks, J. R. Bargar, T. G. Spiro, J. R. Hein, and A. D. Anbar (2011), The molecular mechanism of Mo isotope fractionation during adsorption to birnessite, *Geochim. Cosmochim. Acta*, 75, 5019–5031.
- Ziegler, P. A. (1982), *Geological Atlas of Central and Western Europe*, 130 pp., Shell International Petroleum Maatschappij B.V., Amsterdam.